Ab initio calculation of extended x-ray-absorption fine structure in Br_2

S. -H. Chou,* J. J. Rehr, and E. A. Stern
Department of Physics, University of Washington, Seattle, Washington 98195

E. R. Davidson†
Department of Chemistry, University of Washington, Seattle, Washington 98195
(Received 2 September 1986)

A quantitative theory of extended x-ray-absorption fine structure (EXAFS) in diatomic molecules is presented and tested by *ab initio* calculations in Br_2. The theory, based on a refinement of conventional EXAFS theory, takes into account (1) an energy-dependent exchange-correlation potential, (2) multielectron excitations, and (3) a single-scattering, spherical-wave expansion. Inelastic processes are included assuming that core-hole excitations and losses in propagation are uncorrelated. We find that a Dirac-Hara exchange potential gives better overall agreement of the EXAFS phase than does the Hedin-Lundqvist potential. The amplitude discrepancy between experiment and single-particle theory can be corrected by adding core-hole lifetime effects, experimental resolution, and multielectron excitations.

I. INTRODUCTION

The single-particle theory of EXAFS (extended x-ray-absorption fine structure) has been quite successful in describing the overall shape of the experimental EXAFS spectra both in simple molecules and in a few solids.[1–5] However, there is invariably a discrepancy between the measured and calculated EXAFS amplitudes, calculated amplitudes always being larger.[3,6] For example, Lee and Beni[7] introduced an additional factor 0.62 to make the theoretical amplitude for Br_2 consistent with experiment. Part of this discrepancy was due to experimental error but for the one-electron theory of Lee and Beni a factor of 0.8 is still required.[6] Rehr *et al.*[8] and Lee and Beni suggested that such a discrepancy can be ascribed to certain "multielectron excitations" in the system, which give rise to an energy-dependent amplitude reduction factor. A quantitative understanding of EXAFS amplitudes is important for extending the utility of EXAFS, allowing, for example, more accurate determinations of local coordination numbers.

In this article we present a detailed theory of EXAFS in diatomic molecules that includes many-body effects, which aims to resolve this amplitude discrepancy for the case of Br_2. We have chosen to study Br_2, as it is a comparatively simple, single-distance diatomic system with a tolerable number of electrons for *ab initio* calculations; also good experimental data are available.[6] Our theory is based on the prescription of Ref. 8; it includes many-body effects such as an energy-dependent exchange-correlation potential and multielectron excitations. Moreover, a spherical-wave expansion of the wave functions is employed, instead of the plane-wave approximation,[4] and found to be essential for quantitative agreement.

The outline of this paper is as follows. In Sec. II we briefly review the conventional theory of EXAFS. Section III treats local, density-dependent exchange-correlation potentials (ECP), and Sec. IV, inelastic losses. Section V contains the results of our *ab initio* calculation and Sec. VI, a summary and conclusions.

II. EXAFS THEORY

As the single-particle theory of EXAFS has been treated in detail previously by many workers.[4,5,9,10] we only quote the main results here. The normalized EXAFS spectrum χ is defined as the oscillatory part of the x-ray-absorption coefficients μ:

$$\chi=(\mu-\mu_0)/\mu_0 , \tag{2.1}$$

where μ_0 is the smooth absorption coefficient due to an isolated atom. In the one-electron approximation, μ is calculated using the golden rule together with the dipole approximation:

$$\mu\sim\sum_f |\langle\phi_f|\hat{\epsilon}\cdot\mathbf{r}|\phi_i\rangle|^2\delta(E_f+E_i-\hbar\omega) , \tag{2.2}$$

where $|\phi_i\rangle$ and $|\phi_f\rangle$ refer to one-particle eigenstates with energies E_i and E_f, respectively, of effective one-electron Hamiltonians appropriate to the initial and the final states and $\hat{\epsilon}$ is the x-ray polarization vector.

For a diatomic molecule and K-shell absorption, the single scattering approximation to the final state yields a spherical wave expansion for χ:

$$\chi=\mathrm{Im}ke^{2i\delta_1^c}\sum_{L,L'}e^{i\delta_l}\sin\delta_l\,|C_{10,L'L}|^2h_{l'}^{(+)2}(kR)e^{-2\sigma^2k^2} , \tag{2.3}$$

where the wave number k is

$$k=\sqrt{2(\hbar\omega+E_i-E_0)} . \tag{2.4}$$

Here E_0 is the *inner potential*, δ_1^c is the $l=1$ phase shift of the central atom, δ_l the l-wave phase shift of the neighboring atom, L stands for the angular quantum numbers (l,m), $C_{10,L'L}=\int Y_{10}^*(\hat{\mathbf{k}})Y_{L'}(\hat{\mathbf{k}})Y_L(\hat{\mathbf{k}})d\hat{\mathbf{k}}$ are Gaunt coef-

ficients which vanish unless $l'=l\pm1$, and $h_l^{(+)}$ are spherical Hankel functions. In obtaining this expression the polarization vector has been taken along the z axis and an average over all molecular orientations carried out. The Debye-Waller factor $e^{-2\sigma^2k^2}$ is due to the mean-square fluctuation in bond length. For diatomic systems multiple-scattering corrections are of third and higher order in the scattering amplitude and thus can safely be neglected. In the small-atom and short-wavelength limit,

$$h_l^{(+)}(kR)\simeq\frac{e^{i(kR-l\pi/2)}}{kR}\ ,\quad kR\gg l(l+1)\ , \tag{2.5}$$

and Eq. (2.3) reduces to the *plane-wave approximation* (PWA);

$$\chi=\frac{-|f_\pi(k)|}{kR^2}e^{-2\sigma^2k^2}\sin(2kR+2\delta_1^c+\delta_\pi)e^{-2R/\lambda}\ , \tag{2.6}$$

where $f_\pi(k)\equiv|f_\pi(k)|e^{i\delta_\pi}$ is the backscattering amplitude and λ is the mean free path, $\lambda=\{\mathrm{Im}[k+\delta_1^c/R+\delta_\pi/(2R)]\}^{-1}$.

III. EXCHANGE-CORRELATION POTENTIAL

In the single-particle description of EXAFS, many-body interactions between the photoelectron and other electrons are taken into account through an appropriate complex *optical potential*. This potential consists of two parts:[11,12] a Coulomb or Hartree potential and an exchange-correlation potential. Because the nature of this potential for high-energy excited states is not well established, we have studied three local charge-density-dependent ECP's: the real $X\alpha$ exchange potential $(X\alpha)$,[13,14] the energy-dependent Dirac-Hara (ED) potential,[15,16] used in EXAFS calculations for the first time here, and the Hedin-Lunqvist potential (HL).[7,12,17]

In the $X\alpha$ exchange approximation[13,14] (often used in ground-state calculations) the Hartree-Fock (HF) exchange term is replaced by its statistical average over all occupied spin orbitals and evaluated at the local electron charge density $\rho(\mathbf{r})$; this potential is given by

$$V_{\mathrm{xc}}(\mathbf{r})=-\frac{3\alpha}{2\pi}k_F(\mathbf{r})\ , \tag{3.1}$$

where $k_F(\mathbf{r})=[3\pi^2\rho(\mathbf{r})]^{1/3}$ and α is the adjustable exchange parameter.[14] This approximation has computational advantages in practical calculations compared with the nonlocal HF potential used in several previous EXAFS studies;[3,4,18,19] also the nonlocal HF potential is unstable for angular momentum $l\gtrsim9$.[19] However, as we will see, $X\alpha$ is appropriate only for the ground state. Since it is energy independent, it fails at high energies ($E\geq50$ eV) where exchange effects become small and must be replaced by an energy-dependent exchange-correlation potential, such as Dirac-Hara exchange (ED).[15,16] The Hedin-Lundqvist potential[12,17] is a more complicated, numerically constructed non-Hermitian potential, introduced for EXAFS calculations by Lee and Beni.[7] It incorporates the Sham-Kohn density-functional formalism for excited states[20] within the single-plasmon pole approximation[12,17] of the electron-gas dielectric function. Other potentials have also been suggested. For example, the potential of Beni, Lee, and Platzman[21] applied to Cu, but this approach is difficult to use in practice, and we do not discuss it here. Also a semiclassical approach has been developed by Noguera *et al.*[22] which includes dynamic effects but is not considered here; instead, dynamical effects are treated phenomenologically.

A brief description of the formalism associated with these potentials is now given.[12,23] The main result is that the final-state wave function $\phi_k(\mathbf{x})$ [ϕ_f in Eq. (2.2)] of an electron with momentum k will satisfy a Schrödinger-like equation,

$$[-E_k-\tfrac{1}{2}\nabla^2+V(\mathbf{r})]\phi_k(\mathbf{x})+\int d\mathbf{x}'\Sigma(\mathbf{x},\mathbf{x}';E_k)\phi_k(\mathbf{x}')=0\ , \tag{3.2}$$

where the coordinate $\mathbf{x}$ denotes both space and spin, $\mathbf{x}=(\mathbf{r},s)$, E_k is the energy of the electron, $V(\mathbf{r})$ is the Hartree potential, and Σ is the nonlocal ECP. If the charge density of the system $\rho(\mathbf{r})$ varies slowly compared with the local de Broglie wavelength of the electron (a good approximation for EXAFS), the self-energy Σ can be approximated by a *local* ECP $V_{\mathrm{xc}}(\mathbf{r})$,[17] so that (3.2) becomes

$$[-E_k-\tfrac{1}{2}\nabla^2+V(\mathbf{r})+V_{\mathrm{xc}}(\mathbf{r})]\phi_k(\mathbf{x})=0\ . \tag{3.3}$$

Here E_k is the energy defined relative to the muffin-tin zero (in a solid) or the vacuum level, in atoms and molecules.

The $X\alpha$ approximation for $V_{\mathrm{xc}}(\mathbf{r})$ is given by Eq. (3.1). At high energies, $X\alpha$ exchange overestimates $V_{\mathrm{xc}}(\mathbf{r})$, and one must reexamine the derivation of this term from HF theory to obtain a better approximation. From the HF equation, the exchange term is given by

$$V_{\mathrm{xc}}(\mathbf{r})\phi_k(\mathbf{x})=-\sum_j\int d\mathbf{r}'\frac{1}{|\mathbf{r}-\mathbf{r}'|}\phi_j^*(\mathbf{r}')\phi_k(\mathbf{r}')\times\phi_j(\mathbf{r})\delta_{s_js_k}\ . \tag{3.4}$$

If one approximates $\phi_k(\mathbf{x})$ as a plane wave[17,24] with local momentum $p_j(\mathbf{r})$, $\phi_j(\mathbf{x})=(e^{i\mathbf{p}_j(\mathbf{r})\cdot\mathbf{r}}/\sqrt{\Omega})s_j$, where $p_j(\mathbf{r})=[2E_j+k_F^2(\mathbf{r})]^{1/2}$, $k_F(\mathbf{r})$ is the local Fermi wave vector, Ω is the volume of the system, and s_j a spinor, then Eq. (3.4) gives a local energy-dependent exchange approximation,

$$V_{\mathrm{xc}}(\mathbf{r})=-\frac{3\alpha k_F(\mathbf{r})}{2\pi}\left[1+\frac{1-X_k^2}{2X_k}\ln\left|\frac{1+X_k}{1-X_k}\right|\right]\ , \tag{3.5}$$

where $X_k=p_k(\mathbf{r})/k_F(\mathbf{r})$. A parameter α has been added, such that when the energy is close to the Fermi energy, $V_{\mathrm{xc}}(\mathbf{r})$ reduces to the $X\alpha$ potential. This formula with $\alpha=\frac{2}{3}$ was obtained by Dirac[15] and has been discussed by Hara.[16] Note that when the local momentum $p_k(\mathbf{r})$ is much larger than the local Fermi wave vector $k_F(\mathbf{r})$, Eq. (3.5) reduces to

$$V_{\mathrm{xc}}(\mathbf{r})\sim\frac{k_F^3(\mathbf{r})}{p_k^2(\mathbf{r})}\sim\frac{\rho(\mathbf{r})}{k^2}\ ,\quad k\gg k_F(\mathbf{r})\ . \tag{3.6}$$

Thus for a high-energy photoelectron, instead of being

proportional to $k_F(\mathbf{r})$ or $\rho^{1/3}$, $V_{xc}(\mathbf{r})$ becomes proportional to the local charge density $\rho(\mathbf{r})$, and decreases inversely with energy. We have found that this energy dependence is crucial to a good calculation of EXAFS phase shifts. Moreover, since the potential varies as $\rho(\mathbf{r})$ rather than $\rho(\mathbf{r})^{1/3}$, the spurious step in the potential at the muffin-tin radius is reduced. A drawback of this ECP is that it is Hermitian and hence does not include the energy-loss effects which would give rise to an imaginary absorptive part to the potential.

From the work of Sham and Kohn,[20] and of Hedin and Lundqvist,[12,17] a non-Hermitian ECP can be constructed to describe the propagation of the quasielectron in a free-electron gas, namely,

$$V_{xc}(\mathbf{r}) \simeq \Sigma(p(\mathbf{r}), E - V(\mathbf{r}), \rho(\mathbf{r})) \ . \tag{3.7a}$$

Here Σ is the self-energy of an electron in a homogeneous electron gas with momentum $p(\mathbf{r})$, energy $E - V(\mathbf{r})$, and density $\rho(\mathbf{r})$. Lee and Beni[7] approximate this as

$$V_{xc}(\mathbf{r}) \simeq \Sigma(p(\mathbf{r}), \tfrac{1}{2}p^2(\mathbf{r})) \ . \tag{3.7b}$$

To calculate Σ, Beni and Lee use Eqs. (25.14) and (25.15) of Ref. 12,

$$\mathrm{Re}\Sigma(\mathbf{p},\omega) = -\int \frac{d\mathbf{q}}{(2\pi)^3}\frac{4\pi}{q^2}\frac{f(\mathbf{p}+\mathbf{q})}{\epsilon(q, \frac{1}{2}(\mathbf{p}+\mathbf{q})^2-\omega)} - \omega_p^2 \int \frac{d\mathbf{q}}{(2\pi)^3}\frac{4\pi}{q^2}\frac{1}{2\omega_1(q)}\frac{1}{\omega_1(q)-\omega+\frac{1}{2}(\mathbf{p}+\mathbf{q})^2} \ , \tag{3.8a}$$

$$\mathrm{Im}\Sigma(\mathbf{p},\omega) = \frac{\pi\omega_p^2}{2}\int \frac{d\mathbf{q}}{(2\pi)^3}\frac{4\pi}{q^2\omega_1(q)}\{f(\mathbf{p}+\mathbf{q})\delta(\tfrac{1}{2}(\mathbf{p}+\mathbf{q})^2-\omega_1(q)-\omega) - [1-f(\mathbf{p}+\mathbf{q})]\delta(\tfrac{1}{2}(\mathbf{p}+\mathbf{q})^2+\omega_1(\mathbf{q})-\omega)\} \ , \tag{3.8b}$$

where the dielectric function is approximated as

$$\epsilon(q,\omega)^{-1} = 1 + \frac{\omega_p^2}{[\omega^2-\omega_1^2(q)]} \ , \tag{3.9a}$$

$$\omega_1^2(q) = \omega_p^2 + \epsilon_F^2[\tfrac{4}{3}(q/k_F)^2 - (q/k_F)^4] \ , \tag{3.9b}$$

and $f(\mathbf{k})$ is the Fermi distribution function.[12] We have attempted to find analytical expressions for Eqs. (3.8a) and (3.8b) which can well approximate Σ without the need for numerical integration. This is a great simplification in numerical calculations. The analytical formulas we have used to interpolate Σ are[23]

$$\mathrm{Re}\Sigma(p(\mathbf{r}), \tfrac{1}{2}p^2(\mathbf{r})) = -\frac{3\alpha}{2\pi}\left[k_F(\mathbf{r}) + \frac{k_F^2(\mathbf{r})-p^2(\mathbf{r})}{2p(\mathbf{r})}\ln\left|\frac{p(\mathbf{r})+k_F(\mathbf{r})}{p(\mathbf{r})-k_F(\mathbf{r})}\right| + \frac{3\omega_p[p^4(\mathbf{r})-k_F^4(\mathbf{r})]}{p^5(\mathbf{r})}\right] \ , \tag{3.10a}$$

$$\mathrm{Im}\Sigma\left[p(\mathbf{r}), \frac{p^2(\mathbf{r})}{2}\right] = \frac{\omega_p}{2p(\mathbf{r})}\ln\left|\frac{Q_{\min}F(Q_{\max})}{Q_{\max}F(Q_{\min})}\right| \ , \tag{3.10b}$$

where

$$Q_{\max} = -\tfrac{2}{3}k_F^2(\mathbf{r}) + [4k_F^4(\mathbf{r})/9 + k^4 - 4\omega_p^2]^{1/2} \ , \tag{3.11a}$$

$$Q_{\min} = \omega_p^2(p^2(\mathbf{r}) - \tfrac{1}{3}k_F^2(\mathbf{r}) - p(\mathbf{r})\{\omega_p^2/[p^2(\mathbf{r}) - k_F^2(\mathbf{r})/3]\}^{1/2})^{-1} \ , \tag{3.11b}$$

$$F(x) = 2\left[\omega_p^2\left[\frac{x^2}{4} + \frac{k_F^2(\mathbf{r})x}{3} + \omega_p^2\right]\right]^{1/2} + 2\omega_p^2 + \frac{k_F^2(\mathbf{r})x}{3} \ , \tag{3.11c}$$

and $p(\mathbf{r})$ is the electron momentum, defined as[7]

$$p^2(\mathbf{r}) = k^2 + k_F^2(\mathbf{r}) \ . \tag{3.11d}$$

The last term in (3.10a) is very crude but appeared to be adequate in the range $k = 2$–10 a.u. where our calculations are performed. The expression for the imaginary term is a good approximation in the EXAFS region and becomes exact when $p \gg k_F$. Attempts to improve on these approximations are in progress. One can readily see for a low-energy electron ($E \simeq \epsilon_F$) that this ECP reduces to X_α exchange (3.1).

IV. MULTIPLE-ELECTRON EXCITATIONS

A. Multiple-electron excitations in EXAFS

It is known that multiple-electron excitations in the photoabsorption process have a significant influence on the EXAFS amplitude.[7,8,23] Such *intrinsic* losses are not explicitly included in the conventional single-particle formulation, which includes only extrinsic losses through the imaginary part of the potential; however, intrinsic losses have been included phenomenologically through an *ad hoc* constant reduction factor.[7] In this section we outline how

such multiple-electron excitations are included in our theory;[8,23] possible corrections to the sudden approximation are also discussed.

In the single-particle theory outlined in Sec. II, we only considered photoelectrons in the "primary channel," in which the ion with the $1s$ hole is in its fully relaxed ground ionic state. In the sudden approximation, the probability that the final N-particle state (denoted by a prime), $|\Psi'_n\rangle$, consists of a photoelectron in state $|\phi'_{k_n}\rangle$ and the ion with the core hole in its nth excited state $|\Phi_n'^{(N-1)}\rangle$ is given by[25]

$$S_n^2 = |\langle \Phi_i^{(N-1)} | \Phi_n'^{(N-1)} \rangle|^2 , \tag{4.1}$$

i.e., the square of the overlap between the passive electrons in the initial and final $(N-1)$-particle ground states. Here ΔE_n is the excitation energy of the ion and $k_n = (k^2 - 2\Delta E_n)^{1/2}$ is the shifted wave number. By summing over the contribution to the EXAFS from each of these channels, we obtain an expression for the absorption coefficient given by[8]

$$\mu = \sum_n |\langle \phi'_{k_n} | \hat{\epsilon}\cdot\mathbf{r} | 1s \rangle|^2 S_n^2 . \tag{4.2}$$

Hence, by Eq. (2.1), the EXAFS is given by

$$\chi(k) = \sum_n S_n^2 \chi_n(k) , \tag{4.3}$$

where the moment we have assumed that $\sum_n S_n^2 = 1$ [but see Eq. (4.7) below]. For low-energy excitations, χ_n may be approximated as $\chi_0(k_n)$, and Eq. (4.3) for χ can be expressed as a phasor sum. The sum is equivalent in form to the conventional EXAFS formula,[8] but with an energy-dependent amplitude reduction factor:

$$\chi(k) = A(k)\chi_0(k + \phi/2R) , \tag{4.4}$$

where

$$A(k)e^{i\phi} = \sum_n S_n^2 e^{i\phi_n(k)} \tag{4.5}$$

and

$$\phi_n(k) = 2R(k_n - k) . \tag{4.6}$$

B. Corrections to sudden approximation

The *intrinsic* multielectron excitations in EXAFS can be viewed as transitions of passive electrons induced by the creation of the core-hole potential. When the photoelectron has an energy far above threshold, the excitation probability is given by the sudden approximation, Eq. (4.1). Conversely, as the photoelectron energy is reduced toward threshold, one might expect the transition to become more adiabatic and hence that multiple-electron excitations should be suppressed. Indeed, when the final photoelectron energy is below the first excitation energy, there can be no multiple-electron excitations. The nature of the crossover from sudden to adiabatic behavior is an interesting theoretical question which is not yet well understood. Some energy dependence arises naturally within ΔSCF-HF (delta self-consistent-field Hartree-Fock) theory if one does not factorize the final state as $|\phi'_{k_n}\rangle |\Phi_n'^{(N-1)}\rangle$, but rather uses the full Slater-determinant wave functions.[26] However, this goes well beyond the treatment here. Our approach is simply to retain the general form for the absorption coefficient [Eq. (4.2)] but with S_n^2 now energy-dependent excitation probabilities which crudely take the anticipated corrections to the sudden approximation into account. In addition to the sudden approximation (model *a*), we have therefore used a form (model *b*) based on a semiclassical approach and adiabatic perturbation theory[23,27] and also a simple exchange model (model *c*).[23,26]

$$S_n^2 = \frac{P_n}{\sum_m{}' P_m} , \tag{4.7}$$

$$P_n = |\langle \Phi_i^{(N-1)} | (\Phi')_n^{(N-1)} \rangle|^2 , \tag{4.8a}$$

$$P_n = |\langle \Phi_i^{(N-1)} | (\Phi')_n^{(N-1)} \rangle|^2 \frac{4\sin^2(\Delta E_n \tau/2)}{(\Delta E_n \tau)^2} , \tag{4.8b}$$

$$P_n = |\langle \Phi_i^{(N-1)} | (\Phi')_n^{(N-1)} \rangle|^2 \left[1 - \left[\frac{\Delta E_n}{E_k}\right]^2\right]^2 , \tag{4.8c}$$

where the prime in Eq. (4.7) indicates that the sum is restricted to excitations for which $\Delta E_n \le E_k$, E_k being the maximum photoelectron energy. The parameter τ in Eq. (4.8b) is a phenomenological turn-on time, adjusted to fit experiment. We also will present results by using the theory suggested in Ref. 28. Comparisons between the above models and experiments are presented in the following section.

V. CALCULATION AND RESULTS

A. Muffin-tin model

The construction of the ground-state occupied (passive) one-particle states, both with and without the core hole, is based on the $X\alpha$ scattered wave formalism.[29] In this formalism the molecular potential of Br_2 is taken to be a spherically averaged muffin-tin potential within a sphere of radius R_{MT} and beyond an "outer sphere" of radius R_0 centered on the molecule, while the interstitial potential is approximated by a constant V_{MT}. In our calculation of the final states, the central atom is taken to be a relaxed $1s$ core-hole state,[4] with a hole localized at one atomic site.[30]

The self-consistent-field (SCF) procedure starts from an initial potential constructed from superimposed atomic and ionic (i.e., with a $1s$ core hole) potentials, where the corresponding atomic charge densities are determined from (Herman-Skillman-Hartree-Fock-Slater) calculations.[31] The interatomic distance for the ground state is 4.31 a.u.,[32,33] and an "atomic number radii" method suggested by Norman[34] is used to determine the muffin-tin radii for the atomic spheres and for the outer sphere. Choosing the muffin-tin radius at 88% of the atomic number radius, the virial theorem $V = -2T$ is satisfied approximately, and both the ionization energy and transition energy are in agreement with experiment. Thus we set the atomic muffin-tin radius at 2.74 a.u. and the outer sphere radius at 4.89 a.u. At these values the outer sphere is tangent to the atomic spheres.

The deep molecular core levels are labeled by their atomic conventions ($1s$ to $3d$). The upper valence electron levels are labeled by the nomenclature of the $C_{\infty v}$ point group, which is appropriate for a heteronuclear diatomic molecule. The Slater $X\alpha$ exchange potential [Eq. (3.1)] was used in the self-consistent-field procedure[14,24] with $\alpha=0.706\,06$. The SCF iteration procedure was repeated until the eigenvalue of each spin orbital converged to within 0.000 05 Ry (1 Ry=0.5 a.u.). The electronic energy levels for neutral Br_2 and Br_2^+ ($1s$ hole) are listed in Table I.

From a "transition-state" calculation,[14,35,36] we find that the adiabatic ionization energy for the electron in the uppermost valence level 2π of Br_2 is 10.52 eV, very close to the published experimental result of 10.51 eV,[32] and the virial ratio $-2T/V=0.999\,487$.

B. ECP for excited states

As discussed in Sec. III, a different exchange-correlation potential is used to calculate the excited photoelectron state ϕ_k. We present here results for $X\alpha$, ED, and HL potentials. Figure 1 is a plot of $rV_{xc}(r)$ at $k=4.0$ a.u.; the real part of the HL potential shown here is based on the interpolation formula of Eq. (3.9a); for comparison the Lee-Beni result[7] is also given. We see that the switching-off of the exchange-correlation interaction as the density decreases (with increasing r) is more rapid for the ED potential than for the HL potential. Figure 2 illustrates the switching-off of the ED potential with energy. Figure 3 shows the imaginary part of the HL potential for $k=2.8$, 5.0, and 7.0 a.u. The result for $k=7.0$ from Ref. 7 is also plotted (dashed line) for comparison.

C. Inner potential

The inner potential E_0 is defined here as the energy at which k vanishes: $k=[2(E_k-E_0)]^{1/2}$; where $E_k=\hbar\omega+E_i$ is the photoelectron energy, E_i is the initial core-level energy, and k is the wave number. We therefore set the interstitial constant muffin-tin potential V_{MT} equal to E_0. In our SCF calculation, V_{MT} is found to be 10.15 eV below the vacuum value. The energy difference ΔE between the vacuum and the first peak at the absorption edge (which fixes the position of the vacuum level) is determined by the following procedure: in Br_2, the first unoccupied spin orbital is 4σ, so the first peak should correspond to the transition $1s\rightarrow 4\sigma$, with energy $\hbar\omega_1$ (see Fig. 4), while the $1s\rightarrow$continuum transition energy is $\hbar\omega_2$. Thus $\Delta E=\hbar\omega_2-\hbar\omega_1$ or

$$\Delta E=E^T(n_{1s}-1,n_{4\sigma}=0)-E^T(n_{1s}-1,n_{4\sigma}=1)\ , \tag{5.1}$$

where E^T is the total energy of the system and n_i is the occupation number of the ith level. Thus, ΔE is the ionization energy of the 4σ spin orbital in a $1s$ core-hole ground state. We used a transition-state method[14,35,36] to estimate this energy and find that $\Delta E=8$ eV (Fig. 4). (This is different from the value 13 eV used by Kincaid.[3,19]) Since the muffin-tin zero is 10 eV below the continuum limit, we set E_0 at $10-8=2$ eV below the first peak.

D. Phase shifts

The partial-wave phase shifts $\delta_l(k)$ are determined in the usual way by matching at R_{MT},[25]

$$\tan\delta_l(k)=\frac{kj_l'(kr)-\gamma_l j_l(kr)}{kj_l'(kr)-\gamma_l\eta_l(kr)}\ ,$$

$$\gamma_l=\frac{1}{\phi_l(r)}\frac{d\phi_l(r)}{dr}\bigg|_{r=R_{MT}}\ , \tag{5.2}$$

and $\phi_l(r)$ is the regular, radial solution of the Schrödinger equation inside the atomic muffin-tin radius. After obtaining the phase shifts, we can calculate the EXAFS spectrum both with a spherical-wave expansion [see Eq. (2.3)] and with the plane-wave approximation [Eq. (2.6)].

TABLE I. Eigenvalues of Br_2^+ and Br_2 (Ry). ($R_{MT}=2.74$ a.u.; $R_0=4.89$ a.u.)

Level	Br_2^+	Br_2
Br^+ $1s$	−992.1860	
Br $1s$	−961.9932	−961.4534
Br^+ $2s$	−131.2716	
Br $2s$	−124.1967	−123.6594
Br^+ $2p$	−120.7441	
Br $2p$	−112.1589	−111.6213
Br^+ $3s$	−19.0770	
Br $3s$	−17.4017	−16.8663
Br^+ $3p$	−14.9322	
Br $3p$	−13.1786	−12.6432
Br^+ $3d$	−6.9751	
Br $3d$	−5.6108	−5.0758
1σ	−2.3382	−1.5905
2σ	−1.9672	−0.7997
3σ	−1.4625	−1.3541
1π	−1.3306	−0.6462
2π	−1.0555	−0.5032
	$V_{MT}=0.7460$	$V_{MT}=-0.3380$

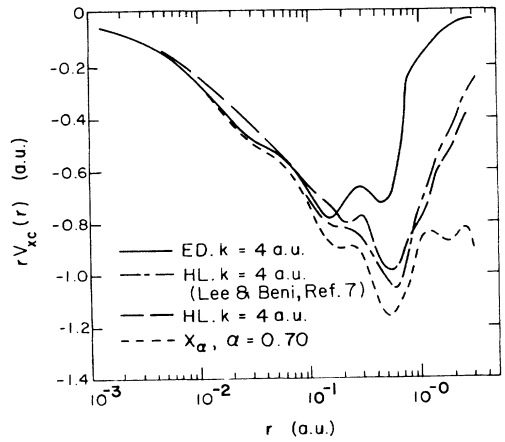

FIG. 1. Plot of $rV_{xc}(r)$ vs r for the neighboring Br atom with electron momentum $k=4.0$ a.u. For the Hedin-Lundqvist potential, only the real part is presented; the results from Ref. 7 are plotted for comparison.

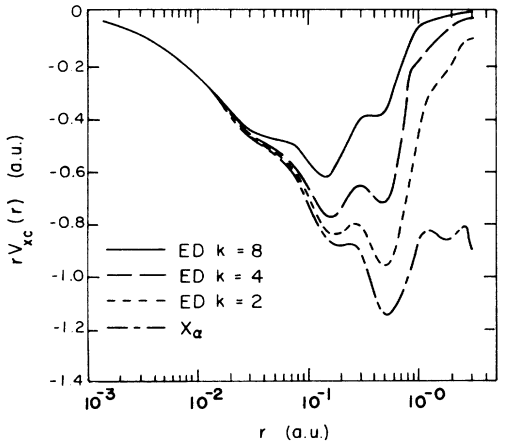

FIG. 2. Plot of $rV_{xc}(r)$ vs r for the neighboring Br atom at electron momenta $k=2.0$, 4.0, and 8.0 a.u. for the energy-dependent Dirac potential (ED). The $X\alpha$ potential is shown for comparison.

One expects that the maximum angular momentum $l_{max} \simeq kb$, where b is the effective range of the force. Since b is of the order of the atomic radius (~ 2 a.u.) or less and $k < 8$ a.u., $l_{max} \simeq 16$; we set $l_{max} = 18$. Convergence was tested by varying l_{max} from 18 to 19, and we found that the backscattering amplitude $f_\pi(k)$ changed only by 0.3% at $k=8$.

For the HL potential, the phase shifts are complex valued, $\delta_l(k) \rightarrow \delta_l(k) + i\beta_l(k)$, and hence the problem of solving the associated coupled second-order differential equations requires complex arithmetic. As a reasonably

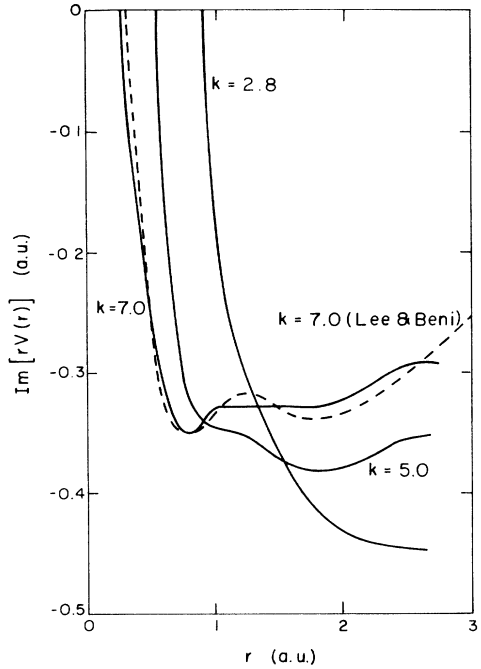

FIG. 3. Plot of $r\,\mathrm{Im}V_{xc}(r)$ vs r for the neighboring Br atom at $k=2.8$, 5.0, and 7.0 a.u. The result from Ref. 7 (dashed line) at $k=7.0$ a.u. is also plotted.

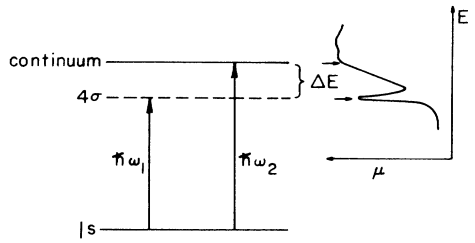

FIG. 4. Plot of the energy location of the first peak of the K-edge x-ray absorption spectrum of Br_2 versus the continuum limit. This serves as a calibration of the inner potential E_0, corresponding to the theoretically determined muffin-tin constant potential V_{MT}.

accurate simplification, we used a WKBJ approximation[37] to determine the imaginary part of the phase shifts:

$$\delta_l(k)+i\beta_l(k) = \int_{r_0}^{R_{MT}} [k^2 - V(r) - V_{xc}(r) - (l+\tfrac{1}{2})^2/r^2]^{1/2} dr - \int_{r_1}^{R_{MT}} [k^2 = (l+\tfrac{1}{2})^2/r^2]^{1/2} dr \,, \quad (5.3)$$

where the turning point $r_1 = (l+\frac{1}{2})/k$ and r_0 is determined by

$$k^2 - V(r_0) - V_{xc}(r_0) - (l+\tfrac{1}{2})^2/r_0^2 = 0 \,. \quad (5.4)$$

The integrals (5.3) were calculated numerically with a mesh size one-third of the original Herman-Skillman mesh[31] to obtain stable results. We also assume that the imaginary part of the HL potential is much smaller than the real part, and solve for $\delta_l(k)$ by using (5.2). As a test of this procedure the real part of the phase shifts $\delta_l(k)$ was calculated from the two methods (matching and WKBJ). The results (Fig. 5) agree with each other for energies above 50 eV for $l < 9$. From our results at $k=2$, 4, and 6 a.u., we find $\beta_1(k) = 0.106$, 0.115, and 0.090, respectively, for the central atom. This is somewhat smaller than the results of Lee and Beni:[7] 0.144, 0.133, and 0.099, respectively. The reason for this difference is that Lee

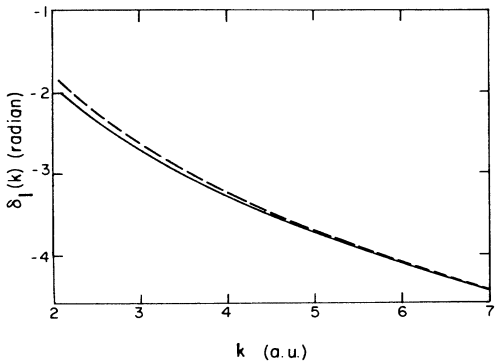

FIG. 5. Comparison of the real part of the phase shifts $\delta_l(k)$ for the neighboring Br atom using the HL potential, as obtained by solving the radial Schrödinger equation (solid line) and by the WKBJ approximaton (dashed line) [see Eqs. (5.2) and (5.3)].

and Beni used an atomic muffin-tin radius larger than ours, and therefore included more (perhaps excessive) damping. Figure 6 is a plot of $\beta_1(k)$ for the neighboring Br atom.

Figure 7(a) shows the comparison of the EXAFS phase for the three ECP treated here using the full spherical wave expansion together with a comparison to experimental results.[6,38] It is clear that the phase using the ED potential with a spherical wave expansion is in very good agreement with experiment without any adjustable parameters! In Fig. 7(b), based on the plane-wave approximation, only the phase from the HL potential is consistent with experiment and this agreement[7] must be regarded as fortuitous.

E. Multielectron excitations

The quantities needed in evaluating the amplitude reduction factor are the overlap integrals between Slater determinant wave functions,

$$|\langle\Phi_i^{(N-1)}|\Phi_n'^{(N-1)}\rangle|^2 = \det\left[\sum_{l=1}^{N-1}\langle\phi_i'^{(n)}|\phi_l\rangle\langle\phi_l|\phi_j'^{(n)}\rangle\right], \quad (5.5)$$

where the prime denotes orbitals for the final configuration with a $1s$ core hole. We approximate the excitation energy ΔE_n for a particle-hole excitation between levels a' and b' as the difference of the corresponding one-electron eigenvalues, i.e.,

$$\Delta E_n \simeq E_{b'} - E_{a'} . \quad (5.6)$$

We only calculate the excitation spectrum for those shake-up channels with low excitation energy. As in Ref. 8 the shake-off spectrum is simply approximated by an exponential decay distribution starting from 20 eV. The relaxation energy,

$$\Delta E_R \equiv \langle\Phi_i'^{(N-1)}|H_{N-1}|\Phi_i'^{(N-1)}\rangle - \langle\Phi_i^{(N-1)}|H_{N-1}|\Phi_i^{(N-1)}\rangle , \quad (5.7)$$

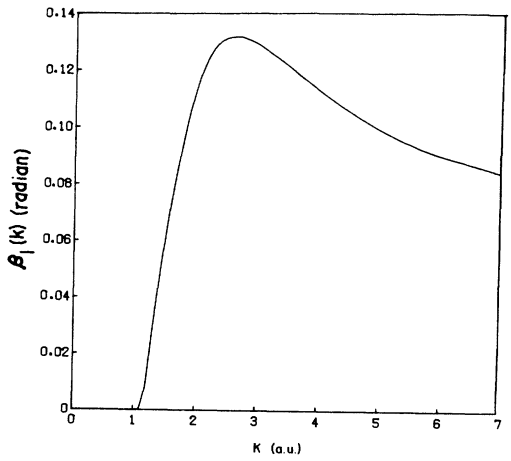

FIG. 6. Plot of the imaginary part of the phase shifts $\beta_1(k)$ for the neighboring Br atom using the HL potential [see Eq. (5.3)].

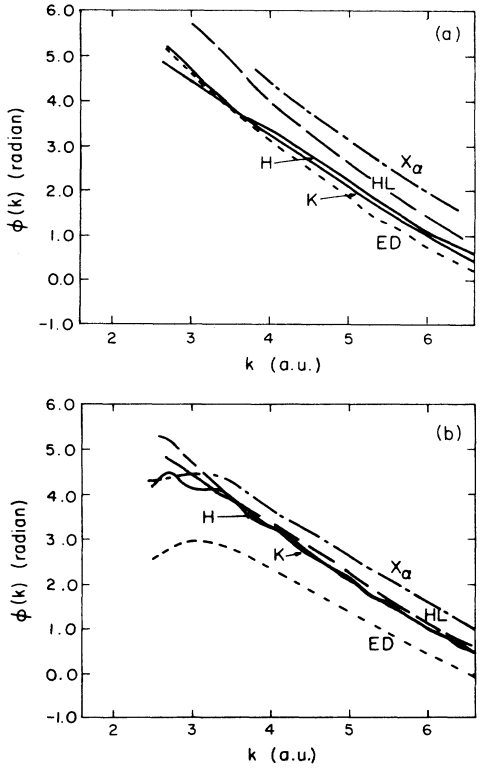

FIG. 7. Overall EXAFS phase $\phi(k)=2\delta_1^c(k)+\delta_\pi(k)$ as calculated using $X\alpha$, HL, and ED potentials, and compared to experiment (K from Ref. 38 and H from Ref. 6). Plot (a) is from the full spherical wave expansion while (b) employs the small-atom—plane-wave approximation. Here $k=0$ is taken at 2 eV below the first peak near the absorption edge.

is found to be 55.8 eV, quite close to the result 50.2 eV of Ref. 39. The average excitation energy (i.e., the centroid of the shake-up—shake-off spectrum) is[40]

$$\Delta E_c = \Delta E_R/(1-S_0^2) = 188 \text{ eV} , \quad (5.8)$$

close to that of Ref. 39, 183 eV.

Table II displays the results of the calculated excitation spectrum for Br_2. We also list results of the photoemission experiment of Bomben *et al.*[41] (Table III). The locations of excitation energies are very similar, but the relative intensities are different, probably because their spectrum is that for a $3d$ hole where correlation effects between $3d$ hole and valence electrons are much stronger than those between $1s$ hole and valence electrons.[42–45] The difference in the shake-off intensities between $1s$ hole

TABLE II. Excitation spectrum for Br_2 ($1s$ photoabsorption).

Peak	Intensity	Energy (eV)
0	0.704	0.0
1	0.066	7.8
2	0.020	14.6
3	0.016	26.5
4	0.009	29.4
5	0.185	shake-off ($E>30$ eV)

TABLE III. Excitation spectrum for Br_2 ($3d$ photoemission[a]).

Peak	Intensity	Energy (eV)
0	0.620	0.0
1	0.064	8.6
2	0.092	16.8
3	0.059	25.0
4	0.045	30.4
5	0.120	shake-off ($E > 33$ eV)

[a]Reference 41.

and $3d$ hole for bromine (0.185 versus 0.12) is consistent with the difference for krypton (0.205 versus 0.122).[46] Our calculation of the overlap factor $S_0^2 = 0.70$ is in good agreement with that of Ref. 39, $S_0^2 = 0.725$. Also the sum of the low-energy molecular overlaps $\sum_n S_n^2$ for $\Delta E_n \leq 30$ eV is 0.815, very close to the atomic overlap factor $S_0^2 = 0.797$. This suggests that the low-lying excitations in a molecule yield a contribution to the EXAFS comparable to that from the central atom, consistent with the experimental results in Ref. 6.

F. EXAFS amplitude

1. Single-particle results

Figure 8 gives a comparison of our calculated backscattering amplitude with that of Teo and Lee.[47] Both are based on the HL potential in the neighboring atom and on the PWA. Figure 9(a) and 9(b) compare theoretical EXAFS spectra for bromine; for comparison, the experimental results[6] are also presented as dotted lines. Here the experimental $\chi(k)$ is obtained using the BrH absorption spectrum as the smooth "atomic" background. It is assumed that any EXAFS oscillations from the H atom are entirely negligible above $k = 2$ a.u. The value of σ^2 used in our calculation in the Debye-Waller factor is $\sigma^2 = 7.084 \times 10^{-3}$ a.u.,[48] assuming an experimental temperature of 300 K. Comparing Figs. 9(a) and 9(b), one sees that the amplitudes of EXAFS obtained with a spherical-wave expansion or with the PWA are obviously quite different. Our results indicate that, as pointed out by Lee and Pendry,[4] the errors in the PWA are quite large

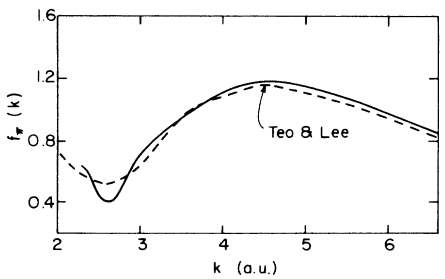

FIG. 8. Comparison of the backscattering amplitude $f_\pi(k)$ for this work (solid line) with that of Teo and Lee (Ref. 47) (dashed line). Both are based on the HL potential and are in good agreement for $k > 3$ a.u.

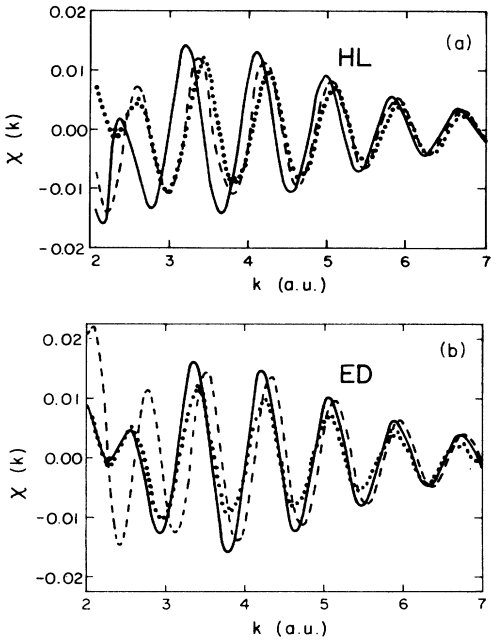

FIG. 9. Comparison of theoretical and experimental EXAFS spectra for Br_2. Theoretical spectra [(a) and (b)] are displayed for both the spherical wave expansion (solid line) and the small-atom—plane-wave approximation (dashed line). Experimental data (dotted lines) are from Ref. 6.

for a low-energy photoelectron ($E < 200$ eV). This partly explains the discrepancies in comparisons between experiment and the conventional EXAFS theory at low energy.[6] We find that it is essential to drop the PWA to get good agreement for both phase and amplitude at energies below 200 eV.

2. Amplitude reduction factor $A(k)$

The single-particle calculations of the EXAFS amplitude including intrinsic losses with the HL potential in both central and neighboring atoms[23] are seen to be only slightly larger (about 10%) than experiment. Thus the effect of multiple-electron excitations due to intrinsic processes in Br_2 is not large. The amplitude reduction factor $A(k)$, as defined in Eq. (4.5), is determined by the excitation probabilities S_n^2. In addition to the sudden approximation, Eq. (4.8a), we used the two different expressions in Eqs. (4.8b) and (4.8c) to interpolate the excitation probability between the adiabatic and sudden approximation limits. All of these require knowledge of the excitation spectrum, or equivalently

$$|\langle \Phi_i^{(N-1)} | \Phi_n'^{(N-1)} \rangle|^2 ,$$

as defined in Eq. (5.5). Figure 10 shows the results for $A(k)$ from these different approaches. We calculate $A(k)$ with (a) the sudden approximation [$\tau = 0$, Eqs. (4.5), (4.7), and (4.8a)], (b) the adiabatic approximation with $\tau = 4\bar{r}/v$, and $\bar{r} = 1.5$ a.u. (which fits the data of Ref. 27), (c) "exchange model,"[23,26] and (d) Thomas's model.[28] The corrections to the sudden approximation increase $A(k)$ from around 0.80 to 0.90. The semiclassical result (b) is

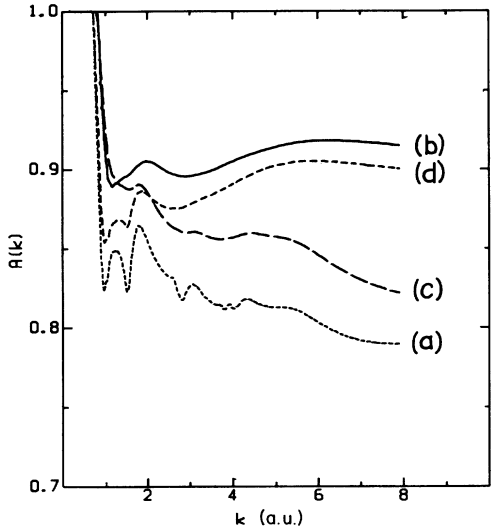

FIG. 10. Amplitude reduction factor $A(k)$ calculated using (a) the sudden approximation [Eq. (4.8a), (b) the adiabatic approximation [Eq. (4.8b)], (c) the exchange model [Eq. (4.8c)], and (d) Thomas's model (Ref. 28) with $r=1.50$ a.u.

consistent with a recent study of Lu and Rehr.[49] This is also qualitatively consistent with experiment.[50] The Ne shake-up satellite peaks were found to be 20—40 % smaller than in the high-energy limit, and the Ar peaks showed some energy dependence.

3. *Damping factor* $e^{-2R/\lambda(k)}$

This damping factor is associated with both the lifetime of the photoelectron and that of the core hole.[10,51,52] These inelastic processes can, in principle, be taken into account by a complex potential. It is found from low-energy electron diffraction (LEED) experiments that this decay can be accounted for by adding a constant imaginary potential (e.g., 4 eV for copper and 9 eV for nickel[53]). Powell[54] found that for most metals, the mean free path $\lambda(k)$ appears to follow a universal curve, which has a minimum at intermediate energies (around 30 eV). For K-edge spectra of Br_2, the total (Lorentzian) linewidth at threshold is about $\Gamma=5.4$ eV (2.7 eV of core-hole lifetime,[55] and the rest for monochromator resolution[19]). This broadening can be lumped into a complex potential with an imaginary part of $\Gamma/2=2.7$ eV. The damping factor associated with the lifetime of the photoelectron is automatically included in the Hedin-Lundqvist potential. Since the ED potential is real, we have also included an energy-dependent imaginary potential V_I to account for damping in this case, namely,

$$V_I=V_0\frac{E}{E+250\text{ eV}}\ , \tag{5.9}$$

where $V_0=9$ eV for Br and E is the photoelectron energy. Note that when the energy is much smaller than 250 eV that the damping factor approaches unity, as expected. This gives a λ comparable to the HL value as shown in Fig. 11.

To assess the role of inelastic effects, we have calculated the EXAFS amplitude with both the damping factor and the amplitude reduction factor included. Three different prescriptions to account for inelastic effects are summarized below.

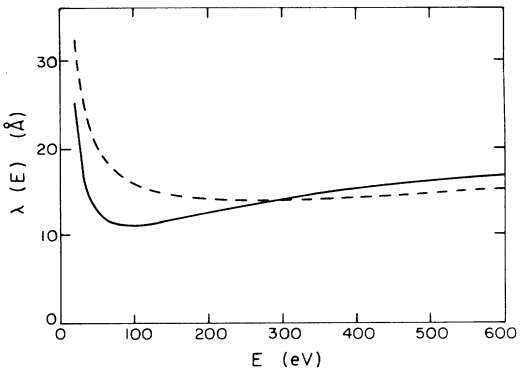

FIG. 11. Plots of the mean free path $\lambda(k)$ for (a) the HL potential (solid line) and (b) the ED potential with a constant imaginary potential V_I [Eq. (5.9)].

(i) Intrinsic losses are ignored and extrinsic losses are calculated from the constant imaginary potential in Eq. (5.9), yielding an overall amplitude

$$F^{(a)}(k)=F_{\rm ED}(k)e^{-2R/\lambda(k)}\ , \tag{5.10a}$$

where $F_{\rm ED}(k)$ is the amplitude obtained from the ED potential and $\lambda(k)$ is the mean free path.

(ii) Intrinsic losses included using the sudden approximation Eq. (4.8a) and extrinsic losses using the mean free path from the imaginary potential in Eq. (5.9), yielding

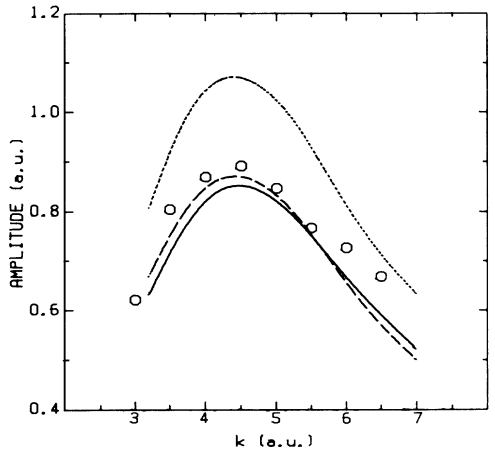

FIG. 12. Overall EXAFS amplitude for Br_2 as calculated from (a) the ED potential with an added constant imaginary potential [Eq. (5.9), dotted line]. (b) Same as (a) except that the amplitude reduction factor $A_{\tau=0}(k)$ obtained from the sudden approximation approach is also included [see Eq. (4.8a) and Fig. 9(a), dashed line]. (c) Intrinsic losses are treated using Eq. (4.8b), using the HL potential only in the backscattering atom, and the core hole lifetime and monochromator resolution effects are lumped into a damping factor $e^{-2R/\lambda_c(k)}$ (solid line). Experimental data (Ref. 6) are indicated by circles (○).

$$F^{(b)}(k)=F_{\mathrm{ED}}(k)A_{\tau=0}(k)e^{-2R/\lambda(k)} . \quad (5.10b)$$

(iii) Intrinsic losses are treated using Eq. (4.8a) and inelastic losses using the HL potential only in the backscattering atom,[7] yielding

$$F^{(c)}(k)=F_{\mathrm{HL}}(k)A_{\tau}(k)e^{-2R/\lambda_c(k)}e^{-\beta_1(k)} , \quad (5.10c)$$

where $\lambda_c(k)$ is obtained with an imaginary potential of 2.7 eV,[19,55] and $\beta_1(k)$ is the extrinsic losses in the central atom.

Figure 12 shows the overall EXAFS amplitudes $|\chi|$ calculated as described above, and for comparison, the results of experiment. Note that the theoretical results, using Eqs. (5.10b) and (5.10c), are in agreement with experiment to within 10%. However, Eq. (5.10c) is logically more appropriate than Eq. (5.10b), since all the damping terms included in Eq. (5.10c) are based on parameters obtained from other independent experimental results and the theoretically determined multiple-excitation spectrum, Eq. (5.10b), has an *ad hoc* term, the effective mean free path $\lambda(k)$.

VI. SUMMARY AND CONCLUSIONS

We have presented a refined version of EXAFS theory which is in good quantitative agreement both for the EXAFS phase and amplitude. The theory includes both *extrinsic* and *intrinsic* inelastic losses. The results depend on how one partitions the losses between intrinsic and extrinsic effects (ignoring possible interference). Several different prescriptions all give reasonable agreement with experiment. In the single-particle calculations, it is found to be essential that one use a full spherical-wave expansion to get agreement at low photoelectron energies. Also, it is necessary to use an energy-dependent exchange-correlation potential. We have found that the unscreened Dirac-Hara exchange gives better agreement for the EXAFS phase than does the Hedin-Lundqvist potential (for which the Coulomb hole decays very slowly with increasing energy). Additional support for this latter finding can be seen in Pettifer's results for Nb.[56] Further work to clarify these findings in other systems is clearly in order.

By comparing Figs. 12(a), 12(b), and experimental results, it is clear that one must include the intrinsic losses in the theoretical calculations of the EXAFS amplitude. For k above 3 a.u., the simple theory of the sudden approximation and extrinsic losses (without dynamic corrections) can describe the amplitude discrepancy between theory and experiment. Inelastic losses in propagation seem to be well approximated by the imaginary part of the HL potential, provided the multielectron excitations are turned on slowly [as shown in Fig. 12(c)]. However, the theoretical curve [Fig. 12(c)] is around 5% smaller than the experimental value. This is because we used overlapping muffin-tin potentials. It is known that an overlapped muffin-tin model gives a much better description of the potentials in molecules than the nonoverlapped one. However, this overestimates the extrinsic loss in the HL calculations.

Alternately, we have found that for the ED potential, an *ad hoc* imaginary potential can be added (as in LEED) (Refs. 23 and 53) with good results. The reduction factor for the sudden approximation is 0.8, where as a constant factor 0.9 in the HL calculations gives good agreement with experiment. The use of the atomic S_0^2 (Refs. 6 and 57) is seen to be consistent with Eq. (5.10b), where $A_{\tau=0}\simeq S_0^2$ and the mean free path $\lambda(k)$ is a quantity which accounts for both resolution and core-hole lifetime as well as extrinsic losses. The ED potential is found to be superior to the HL potential because it reproduces the phase more accurately. Both ED and HL give comparable amplitude, provided an *ad hoc* λ, as estimated from HL, is added to the ED potential.

*Present address: Department of Physics, Northwestern University, Evanston, IL 60201.

†Present address: Department of Chemistry, Indiana University, Bloomington, IN 47405.

[1]D. E. Sayers, E. A. Stern, and F. W. Lytle, Phys. Rev. Lett. **27**, 1204 (1971).

[2]E. A. Stern, Phys. Rev. B **10**, 3027 (1974).

[3]B. M. Kincaid and P. Eisenberger, Phys. Rev. Lett. **34**, 1361 (1975).

[4]P. A. Lee and J. B. Pendry, Phys. Rev. B **11**, 2795 (1975).

[5]J. E. Müller and W. L. Schaich, Phys. Rev. B **27**, 6489 (1983).

[6]E. A. Stern, S. M. Heald, and B. Bunker, Phys. Rev. Lett. **42**, 1372 (1979).

[7]P. A. Lee and G. Beni, Phys. Rev. B **15**, 2862 (1977).

[8]J. J. Rehr, E. A. Stern, R. L. Martin, and E. R. Davidson, Phys. Rev. B **17**, 560 (1978).

[9]C. A. Ashley and S. Doniach, Phys. Rev. B **11**, 1279 (1975).

[10]J. J. Rehr, in *Extended x-ray Absorption Fine Structure*, edited by R. W. Joyner (Plenum, New York, in press), Chap. 2.

[11]C. J. Joachain, *Quantum Collision Theory* (North-Holland, Amsterdam, 1975), Chap. 20.

[12]L. Hedin and S. Lundqvist, Solid State Phys. **23**, 1 (1969).

[13]J. C. Slater, Phys. Rev. **81**, 385 (1951).

[14]J. C. Slater, *The Self-Consistent Field for Molecules and Solids, Quantum Theory of Molecules and Solids* (McGraw-Hill, New York, 1974), Vol. 4; K. Schwartz, Phys. Rev. B **5**, 2466 (1972).

[15]P. A. M. Dirac, Proc. Cambridge Philos. Soc. **26**, 376 (1930).

[16]S. Hara, J. Phys. Soc. Jpn. **26**, 376 (1967).

[17]L. Hedin and B. I. Lundqvist, J. Phys. C **4**, 2064 (1971).

[18]R. F. Pettifer and P. W. McMillan, Philos. Mag. **35**, 871 (1977).

[19]B. M. Kincaid, Ph.D. thesis, Stanford University, 1974 (unpublished).

[20]L. J. Sham and W. Kohn, Phys. Rev. **145**, 561 (1966).

[21]G. Beni, P. A. Lee, and P. M. Platzman, Phys. Rev. B **13**, 5170 (1976).

[22]C. Noguera, D. Spenjaard, and J. Friedel, J. Phys. F **9**, 1189 (1979).

[23]S.-H. Chou, Ph.D. thesis, University of Washington, 1982; J.

J. Rehr and S.-H. Chou, in *EXAFS and Near Edge Structure,* edited by A. Bianconi, L. Incoccia, and S. Stipcich (Springer-Verlag, Berlin, 1982), p. 22.
[24]N. W. Ashcroft and N. D. Mermin, *Solid State Physics* (Holt, Rinhart and Winston, New York, 1976).
[25]L. I. Schiff, *Quantum Mechanics,* 3rd ed. (McGraw-Hill, New York, 1968), Chap. 8; C. S. Fadley, Chem. Phys. Lett. **25**, 225 (1973).
[26]J. Stohr, R. Jaeger, and J. J. Rehr, Phys. Rev. Lett. **51**, 821 (1983).
[27]T. A. Carlson and M. O. Krause, Phys. Rev. A **140**, 1057 (1965).
[28]T. D. Thomas, Phys. Rev. Lett. **52**, 417 (1984).
[29]K. H. Johnson, Adv. Quantum Chem. **7**, 143 (1973).
[30]P. S. Bagus and H. F. Schaefer, J. Chem. Phys. **56**, 224 (1972).
[31]F. Herman and S. Skillman, *Atomic Structure Calculations* (Prentice-Hall, Englewood Cliffs, 1963).
[32]*Comprehensive Inorganic Chemistry,* edited by A. F. Trotman-Dickinson *et al.* (Pergamon, Oxford, 1973), Vol. 2, p. 23.
[33]G. Herzberg, *Spectra of Diatomic Molecules* (Van Nostrand-Reinhold, New York, 1950).
[34]J. G. Norman, J. Molec. Phys. **31**, 1191 (1975).
[35]J. C. Slater, Adv. Quan. Chem. **6**, 1 (1972).
[36]A. R. Williams, R. A. deGroot, and C. Sommers, J. Chem. Phys. **63**, 628 (1975).
[37]P. M. Morse and H. Feshbach, *Methods of Theoretical Physics* (McGraw-Hill, New York, 1953), Vol. II; J. Knoll and R. Schaeffer, Ann. Phys. (N.Y.) **97**, 307 (1976).
[38]P. H. Citrin, P. Eisenberger, and B. M. Kincaid, Phys. Rev. Lett. **36**, 1346 (1976).
[39]R. L. Martin and E. R. Davidson, Phys. Rev. A **16**, 1341 (1977).
[40]R. Manne and T. Aberg, Chem. Phys. Lett. **7**, 282 (1970).
[41]K. D. Bomben, M. K. Bahl, J. K. Gimzewski, S. A. Chambers, and T. D. Thomas, Phys. Rev. A **20**, 2405 (1980).
[42]T. A. Carlson, *Photoelectron and Auger Spectroscopy,* (Plenum, New York, 1975), Chap. 5.
[43]S. Hufner and G. K. Wertheim, Phys. Rev. B **7**, 2333 (1973).
[44]P. S. Bagus, A. J. Freeman, and F. Sasaki, Phys. Rev. Lett. **30**, 850 (1973).
[45]S. P. Kowalczk, L. Ley, R. A. Pollak, F. R. McFeely, and D. A. Shirley, Phys. Rev. B **7**, 4009 (1973).
[46]T. A. Carlson, C. W. Nestor, Jr., T. C. Tucker, and F. B. Malik, Phys. Rev. **169**, 37 (1968).
[47]B. K. Teo and P. A. Lee, J. Am. Chem. Soc. **101**, 2815 (1979).
[48]S. J. Cyvin, *Molecular Vibrations and Mean Square Amplitudes* (Elsevier, Amsterdam, 1968), Chap. 10.
[49]Dan Lu and J. J. Rehr, in Proceedings of the IVth International Conference on EXAFS and Near Edge Structure (1986) [J. Phys. (Paris) (to be published)].
[50]P. H. Kobrin, Ph.D. thesis, Stanford University, 1983 (unpublished).
[51]G. S. Brown and S. Doniach, in *Synchrotron Radiation Research,* edited by H. Winick and S. Doniach (Plenum, New York, 1980).
[52]F. W. Kutzler, C. R. Natoli, D. K. Misemer, S. Doniach, and K. O. Hodgson, J. Chem. Phys. **73**, 3274 (1980).
[53]J. B. Pendry, J. Phys. C **5**, 2567 (1972).
[54]C. P. Powell, Surf. Sci. **44**, 29 (1974).
[55]This core-hole lifetime was obtained by an interpolation from the data of Table I of L. G. Parratt, Rev. Mod. Phys. **31**, 616 (1959).
[56]R. F. Pettifer and A. D. Cox, in *EXAFS and Near Edge Structure,* edited by A. Bianconi, L. Incoccia, and S. Stipcich (Springer-Verlag, Berlin, 1982), p. 66.
[57]E. A. Stern, B. A. Bunker, and S. M. Heald, Phys. Rev. B **21**, 5521 (1979).